ACS OMEGA

http://pubs.acs.org/journal/acsodf

Article

Enhancing the Rheological and Filtration Performance of Water-Based Drilling Fluids Using Silane-Coated Aluminum Oxide NPs

Imran Ahmed Hullio, Abdul Haque Tunio,* Waseem Akhtar, Muddassir Ali Memon, and Nasir Mehmood Gabol

Cite This: *ACS Omega* 2025, 10, 955–963

Read Online

ABSTRACT: For optimizing the drilling efficiency, nanoparticles (NPs) specifically nanometal oxides have been used in water-based drilling fluids (WBDF). Nano metal oxides improve the rheological and filtration characteristics of the WBDF. However, dispersion instability among pristine nano metals shrinks the performance of the nanometal oxides due to high surface energy. Therefore, this study aims to utilize silane-coated aluminum oxide NPs (S-Al_2O_3) as an alternative to widely used pristine aluminum oxide (P-Al_2O_3) in water-based drilling fluids. The S-Al_2O_3 NPs were synthesized using 3-aminopropyl triethoxysilane (APTES). FTIR, XRD, and SEM analyses were carried out to examine the crystalline structure and surface morphology of NPs. Moreover, the rheological and filtration properties of nanowater-based drilling fluids were investigated at low-pressure and low-temperature (LPLT) conditions. The results of experiments revealed that S-Al_2O_3 NPs significantly upgraded the rheological properties compared to P-Al_2O_3 NPs. The S-Al_2O_3 NPs reduced plastic viscosity from 12.6 to 9.6 cP, apparent viscosity from 34.5 to 26.5 cP, and yield point from 46.5 to 39.5 lb/100 ft^2. The gel strengths (10 s and 10 min) were reduced from 44.5 to 32 lb/100 ft^2 and from 77 to 59 lb/100 ft^2, respectively. Furthermore, S-Al_2O_3 NPs enhanced the filtration performance, achieving a 26% reduction in filtrate loss and forming a thinner, more impermeable mud cake than P-Al_2O_3 NPs. In conclusion, the application of S-Al_2O_3 NPs in water-based drilling fluid was found to be effective in improving the rheological properties and controlling the filtrate loss effectively under LPLT conditions. The utilization of silane-coated NPs used in this study will open new and novel doors of research in the fields of both drilling engineering and nanotechnology.

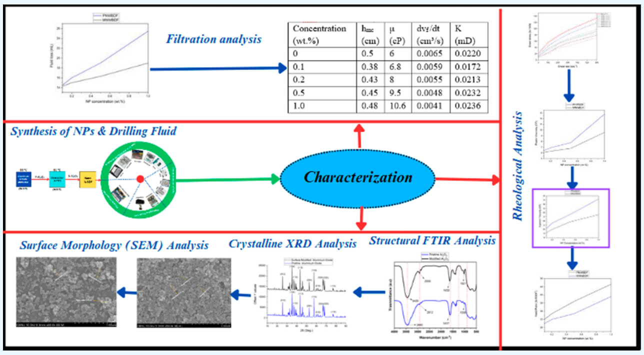

■ INTRODUCTION

In the drilling circulation process, the drilling fluids remove the drilled cuttings, apply the hydrostatic pressure, maintain the wellbore stability, and cool and lubricate the drilling bit.[1,2] Drilling mud is a mixture of variety of liquids, solids, and chemicals depending upon the formation, temperature, and pressure conditions.[3−5] Generally, most additives of the drilling fluid are added to develop the required properties: xanthan gum, lignite, starch, barite, potassium chloride, and polymers.[6−10] Nowadays, nanomaterials are vigorously used in the field of drilling fluid engineering to enhance the performance of drilling fluids and address various challenges in drilling operations. Nanoparticles have a high area-to-volume ratio; therefore, they are highly reactive and perform superior functionality.[11−14] Numerous studies have examined the use of NPs to enhance the performance of the drilling fluids by improving their rheology and filtration.[15−21]

For instance, zinc oxide (ZnO) nanoparticles significantly improved the fluid's rheological and filtration properties of WBDF, reducing the filtration loss volume by 42%, increasing the viscosity by 150%, enhancing the yield strength by 0.8%, and increasing the gel strength by 55% compared to untreated mud.[22] Conversely, copper oxide (CuO) nanoparticles were found to decrease the viscosity by 50%, the yield point by 84%, and the gel strength by 95% at a concentration of 0.5 wt % under high-pressure, high-temperature (HPHT) conditions while also reducing the fluid loss volume by approximately 30%. However, higher NP concentrations led to thicker filter cakes on the wellbore walls due to particle agglomeration.[23] Similarly, iron oxide (Fe_2O_3) nanoparticles showed a 27% increase in viscosity, a 1.61% increase in yield strength, and a 100% increase in gel strength, along with significant improvements in fluid loss and mud cake thickness compared to mud

Received: September 3, 2024
Revised: December 7, 2024
Accepted: December 10, 2024
Published: December 19, 2024

https://doi.org/10.1021/acsomega.4c08116
ACS Omega 2025, 10, 955−963

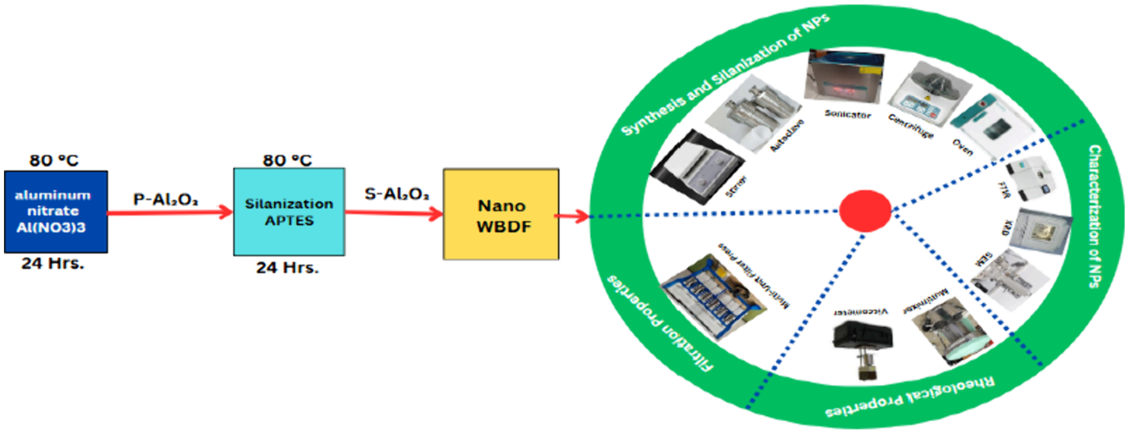

Figure 1. Conceptualized schematic of experiments of research.

without NPs.[24] A comparative study involving four nanometal oxides—aluminum oxide (Al_2O_3), titanium dioxide (TiO_2), silicon dioxide (SiO_2), and CuO—was conducted, and results exhibited that nanoaluminum oxide increased the filtration loss volume by 80% while SiO_2, TiO_2, and CuO nanoparticles reduced the filtration loss volume. Additionally, Al_2O_3, TiO_2, and CuO nanoparticles improved the rheological properties of bentonite WBDF compared to the base mud.[25]

Furthermore, the modified Fe_3O_4/PSSS NP study revealed that Fe_3O_4/PSSS NPs effectively controlled fluid loss by 30% and enhanced the rheological properties of WBDF against its pristine counterpart NPs.[26] Additionally, surface-modified silicon oxide nanoparticles (SiO_2/PAMPS, poly(2-acrylamide-2-methylpropanesulfonic acid)) effectively blocked micro- and nanopores in the wellbore, significantly reducing filtration loss by 55% under both low-pressure, low-temperature (LPLT) and HPHT conditions in comparison to pristine SiO_2 NPs.[27,28]

As mentioned above, the surface-modified metal oxides show greater performance in improving the rheological and filtration properties of the WBDF than the pristine nano metal oxides. The pristine nano metal oxides have greater agglomeration properties due to their high surface energy; therefore, they have high dispersion instability. In comparison, the surface-modified nanometal oxides have high anti-agglomeration properties because their surface energy is controlled by coupling a functional organic group; hence, they show greater dispersion stability. The novelty of this research lies in the surface modification of pristine nano aluminum oxides through a silanization technique by attaching APTES with P-Al_2O_3NPs to improve their dispersion stability. The purpose of this research is to examine and compare the rheological and filtration properties of WBDF with pristine nano aluminum oxide (P-Al_2O_3) and silane-coated nano aluminum oxide (S-Al_2O_3). To achieve this, P-Al_2O_3 nanoparticles were synthesized and characterized, and their surfaces were modified through silanization. Subsequently, the WBDF was prepared, and varying quantities of both types of nanoparticles were incorporated into the base mud.

■ EXPERIMENTAL SECTION

Materials. The chemical materials and compounds utilized in this study for the synthesis of P-Al_2O_3 and S-Al_2O_3 nanoparticles (NPs) and bentonite water-based drilling fluid are detailed as follows. For the synthesis of P-Al_2O_3 NPs, aluminum nitrate nonahydrate ($Al(NO_3)_3{\cdot}9H_2O$) with a purity of 98% was acquired from Daejung. 3-Aminopropyl triethoxysilane, $H_2N(CH_2)_3Si(OCH_2CH_3)_3$ (APTES), also with a purity of 98%, was obtained from Alfa Aesar for the silanization of the pristine NPs. Bentonite powder with 95% purity and barite ($BaSO_4$) were sourced from Daejung for the preparation of the WBDF.

Methods. The synthesis of pristine aluminum oxide (P-Al_2O_3) NPs and the subsequent silanization of the nanometal oxide were conducted by using a variety of laboratory instruments. These included a hot plate magnetic stirrer (Mtops, MS-300HS), autoclave reactor, sonicator (Faithful, SS-Z410), centrifuge (Hettich, D-78532), furnace (Mtixtl, KSL-1700X-A3), and oven (Faithful, 202-0A). The vibrational frequencies of bonds in the molecule were analyzed through Fourier transform infrared (FTIR) spectroscopy (PerkinElmer, Spectrum Two). Moreover, the crystalline structure and purity of the NPs were verified through X-ray diffraction (XRD) analysis (Siemens, D5000). Furthermore, the surface morphology of the NPs was evaluated by using a scanning electron microscopy (SEM) machine (Hitachi, SU8020). For drilling fluid preparation, a multi-mixer (Sterling Multi, 9B) was employed to ensure the thorough mixing of additives. The rheological and filtration properties of the drilling fluids were measured by using a viscometer (OFITE 800) and a multiunit filter press (OFITE, 140-40). Moreover, a Saybolt viscometer (LabTek, SL-FT-001) was used to measure the kinetic viscosity of the mud filtrate. A general schematic of research experiments is conceptualized in Figure 1.

Synthesis of Pristine Aluminum Oxide NPs. For the preparation of pristine aluminum oxide NPs, a wet chemical process was used. The aluminum nitrate $Al(NO_3)_3$ was placed in deionized (DI) water to create a homogeneous solution. The solution was placed in a sealed autoclave reaction vessel under a controlled temperature of around 80 °C and the pH of the solution adjusted in the range of 4 to 5. The vessel was placed in an oven at 140 °C for 8 h. After the vessel was heated, the solid particles were filtered, washed with DI water, and dried.

Silanization of Pristine Aluminum Oxide NPs. In this study, the silanization technique was used for the surface modification of pristine nano aluminum oxide. The ethanol and APTES were mixed and stirred for 24 h at room temperature to create a solution. After 24 h of hydrolysis, the aluminum oxide NPs were added to the solution to create the suspension, and the suspension was heated to 80 °C for the

https://doi.org/10.1021/acsomega.4c08116
ACS Omega 2025, 10, 955−963

next 24 h. Afterward, the solution was washed with DI water and finally dried out.

Preparation of Nano Bentonite Water-Based Drilling Fluid. The base mud was prepared by mixing the various materials, and their quantities are shown in Table 1.

Table 1. Water-Based Drilling Fluid Composition

material	concentration
water	350 mL
bentonite	22.5 g
barite	20.3 g
polyanionic cellulose	0.5 g
caustic soda	0.5 g

The same quantities of substances were used consistently across all samples for the base fluid. For the preparation of pristine nano water-based drilling fluid (PNWBDF), 0.1, 0.2, 0.5, and 1.0 wt % of P-Al_2O_3 NPs were added to the base fluid; similarly, the silanized nano water-based drilling fluid (SNWBDF) was prepared by mixing 0.1, 0.2, 0.5, and 1.0 wt % of the S-Al_2O_3 NPs in each sample. All experiments were conducted according to the standards and guidelines of the ASTM and API.

Determination of Rheological Characteristics of WBDF. The rheological parameter (θ) of the drilling fluids was determined by using a rotary viscometer, and this parameter was used to calculate the rheological properties by using the following equations:

$$\mathrm{SS(lb/100ft^2)} = \theta_N \times 1.067 \quad \text{(i)}$$

$$\mathrm{SR(S^{-1})} = N \times 1.703 \quad \text{(ii)}$$

$$\mathrm{AV(cp)} = \theta_{600}/2 \quad \text{(iii)}$$

$$\mathrm{PV(cp)} = \theta_{600} - \theta_{300} \quad \text{(iv)}$$

$$\mathrm{YP(lb/100ft^2)} = \theta_{600} - \mathrm{PV} \quad \text{(v)}$$

$$10_{\mathrm{sec}}\mathrm{gel\ strength(lb/100\ ft^2)} = \theta_3 \text{ after } 10_{\mathrm{sec}} \quad \text{(vi)}$$

$$10_{\mathrm{min}}\mathrm{gel\ strength(lb/100\ ft^2)} = \theta_3 \text{ after } 10_{\mathrm{min}} \quad \text{(vii)}$$

where SS is the shear stress, SR is the shear rate, AV is the apparent viscosity, PV is the plastic viscosity, YP is the yield point, θ_N is the dial reading, and N is the rotary speed (rpm).

Determination of Filtration Characteristics of WBDF. A multiunit filter press was used to investigate the filtration rate and mud cake thickness at the LPLT conditions, specifically at 100 psi and 27 °C. This equipment, which includes a pressurized cell equipped with a filter medium, was used to determine filtrate loss and evaluate the properties of the filter cake. A nitrogen gas cylinder was connected to the filter press to maintain the required pressure of 100 psi.

■ RESULTS AND DISCUSSION

Characterization of P-Al_2O_3 and S-Al_2O_3 NPs. The FTIR analysis of the P-Al_2O_3 and S-Al_2O_3 NPs reveals characteristic absorption peaks corresponding to distinct functional groups and bonding features, as shown in Figure 2. Peaks at 607 and 756 cm^{-1} confirm Al−O bond stretching, while 1008 and 1109 cm^{-1} relate to Al−O−H bending.[28−30] A broad O−H band around 3420 cm^{-1}, along with a bending mode at 1640 cm^{-1}, reflects H_2O vibration modes.[31] Al−O−Si and Si−O−Si bonds, possibly due to a silane coupling agent, appear between 980 and 1220 cm^{-1}.[32] A wide peak from 3000 to 3550 cm^{-1} confirms adsorbed water on the Al_2O_3 surface.[33] Additionally, APTES exhibit peaks at 1600 and 2950 cm^{-1}, with the 1632 cm^{-1} peak indicating N−H vibrations and 2935 cm^{-1} showing C−H stretching, confirming the presence of the silane coupling agent on treated surfaces.[34]

The XRD diffraction peaks are used to confirm the structure of the crystals and their purity according to the corresponding crystal planes. Figure 3 shows the indexes for the diffraction

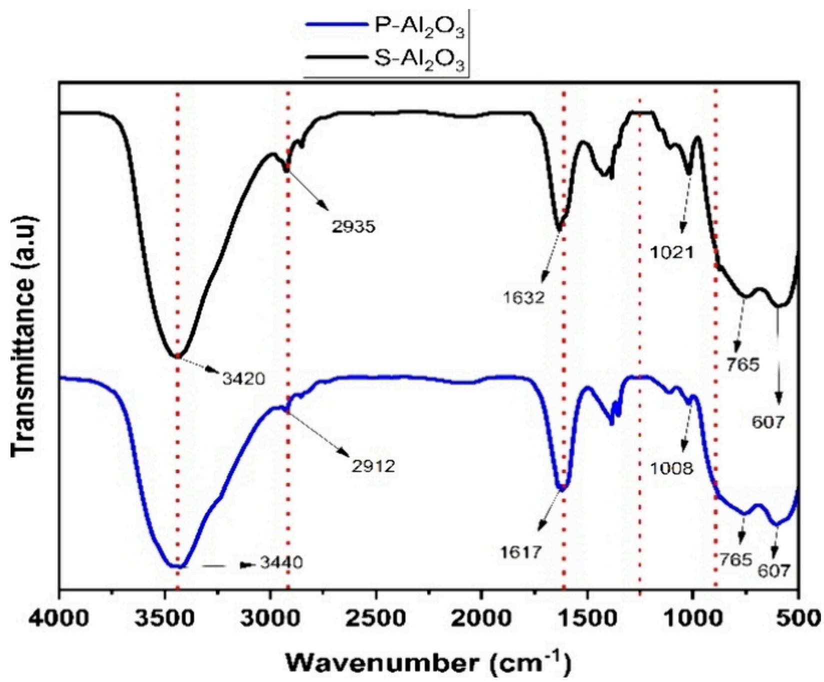

Figure 2. FTIR analysis of P-Al_2O_3 and S-Al_2O_3 NPs.

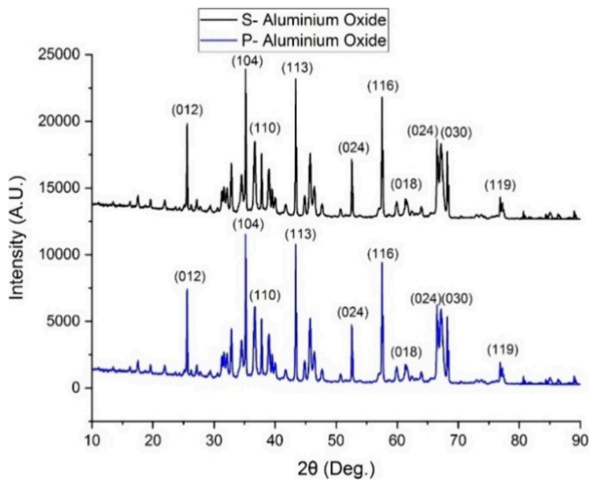

Figure 3. XRD analysis of P-Al_2O_3 and S-Al_2O_3 NPs.

peaks at the corresponding planes 2θ = 25.6, 35.1, 43.3, 52.5, 57.4, and 66.5, which are (104), (110), (113), (116), (119), and (030), respectively, for the P-Al_2O_3 NPs.[35−37] Similarly, the XRD results of the silane-coated Al_2O3 NPs show the same XRD peaks and planes, which shows that there is no change in the crystal structure of NP. The XRD results show that P-Al_2O_3 and S-Al_2O_3 NPs have polycrystalline and rhombohedral crystal structures. The Debye−Scherrer formula is used to calculate the crystallite size of the NPs, which is 33.49 nm.

The surface morphology of the P-Al_2O_3 and S-Al_2O_3 NPs was analyzed by using SEM. The SEM images show that the surface morphology of P-Al_2O_3 and S-Al_2O_3 NPs is nanoplate, as shown in Figures 4 and 5, respectively. The whitish part in Figure 5 shows the silane (APTES) coating over the Al_2O_3 NPs.

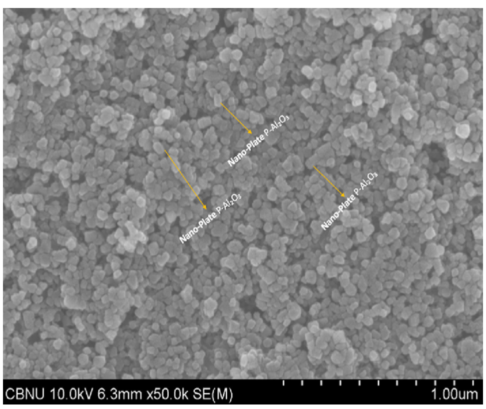

Figure 4. Surface morphology of P-Al_2O_3 NPs.

Effect of NPs on the Rheological Characteristics of WBDF. *Shear Stress vs Shear Rate.* Figure 6 shows the phenomenon of agglomeration and dispersion of the P-Al_2O_3 and S-Al_2O_3 NPs in the drilling fluid.

The shear stress (SS) and shear rate (SR) of WBDF, PNWBDF, and SNWBDF were evaluated by using a viscometer. As depicted in Figure 6, the increase in shear stress with shear rate indicates that the flow behavior of the base mud confirms the Herschel−Bulkley model, exhibiting shear-thinning or pseudoplastic properties akin to Bingham pseudoplastic fluids.[38,39]

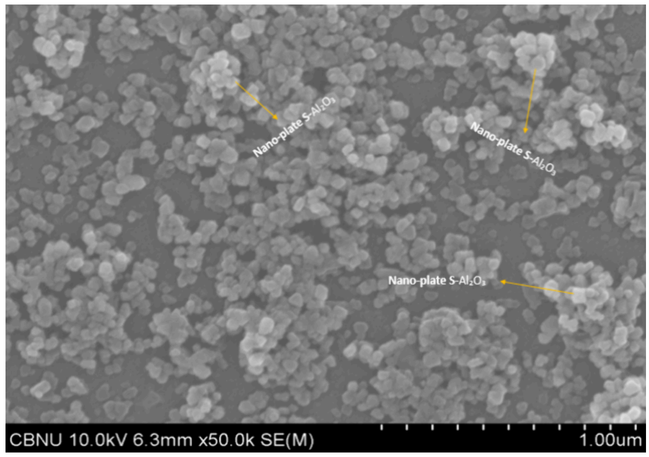

Figure 5. Surface morphology of S-Al_2O_3 NPs.

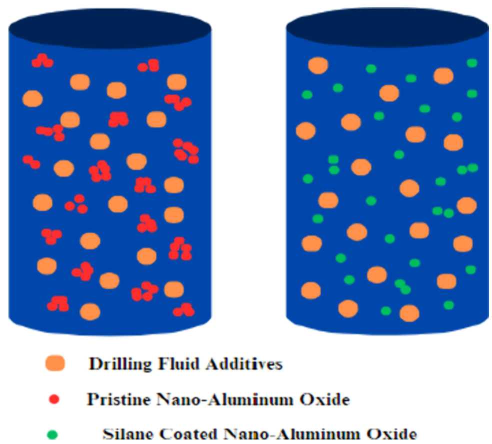

Figure 6. Dispersion of NPs in drilling fluids.

Figure 7 illustrates that SNWBDF exhibits a greater degree of shear thinning compared to PNWBDF. This enhanced

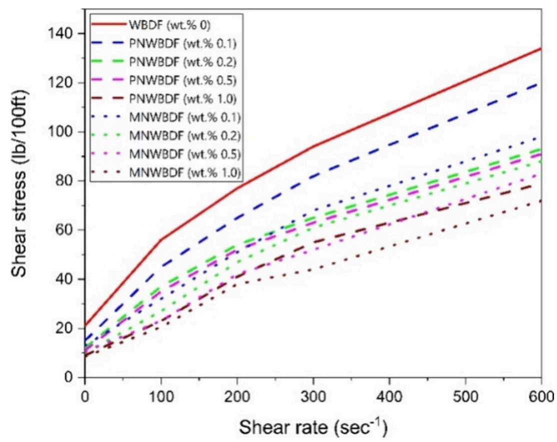

Figure 7. Shear stress vs shear rate of the WBDF, PNWBDF, and SNWBDF.

shear-thinning effect is attributed to the anti-agglomeration properties of the S-Al_2O_3 NPs. The S-Al_2O_3 NPs exhibit superior dispersion stability due to their high electrostatic repulsion, steric hindrance, lower surface energy, weaker van der Waals forces, and minimal Ostwald ripening effect among the NPs.

https://doi.org/10.1021/acsomega.4c08116
ACS Omega 2025, 10, 955−963

Plastic Viscosity. Plastic viscosity (PV) refers to the resistance to flow caused by friction between solid particles within the drilling fluid. Typically, drilling fluids with high PV are more difficult to pump, which can be detrimental to the drilling efficiency. Consequently, achieving the optimal PV is essential for ensuring safe and effective drilling operations.[40]

As illustrated in Figure 8, the PV of the drilling fluid generally increased with the addition of NPs. The P-Al_2O_3 NPs increased the PV of the mud by approximately 25% than did the S-Al_2O_3 NPs at the equivalent concentration. The greater increase in PV with P-Al_2O_3 NPs compared to S-Al_2O_3 NPs can be attributed to the clustering of the pristine NPs due to stronger van der Waals forces.

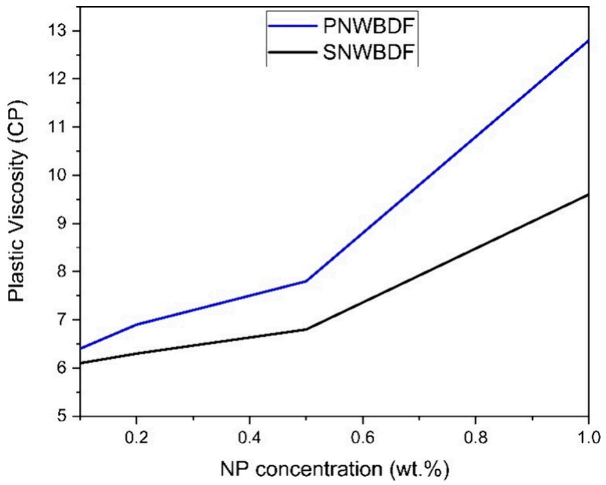

Figure 8. Plastic viscosity at different concentrations of P-Al_2O_3 and S-Al_2O_3 NPs.

Apparent Viscosity. Apparent viscosity is defined as the effective viscosity of a drilling fluid under specific flow conditions, representing the ratio of shear stress to shear rate in a given flow state. The drilling fluids are non-Newtonian; their viscosity changes in response to shear stress, making apparent viscosity a crucial parameter for understanding the flow behavior of the drilling fluid under both static (trip-in) and dynamic (trip-out) conditions.[41]

In this work, the base mud exhibits an apparent viscosity of 18 cP. As depicted in Figure 9, the apparent viscosity of WBDF increases with the addition of NPs. Notably, the apparent viscosity of SNWBDF is 26.5 cP at 1.0 wt % of S-Al_2O_3 NPs, which is almost 30% lower than the apparent viscosity of the PNWBDF at a similar amount of P-Al_2O_3 NPs. This discrepancy is attributed to the dispersion stability of S-Al_2O_3 NPs, which possess a lower surface energy and surface charge than P-Al_2O_3 NPs.

Yield Point. The yield point (YP) can be defined as the resistance to fluid flow caused by surface-charged particles. An increase in YP generally enhances the drilling fluid's capacity to efficiently transport and carry cuttings to the surface. However, the YP must be sufficiently high to ensure the effective removal of cuttings from the wellbore.[42]

In this study, the YP of the base mud was 21 lb/100 ft^2. Figure 10 depicts that the YP of WBDF showed a steady increase with the addition of NPs, at concentrations from 0.1 to 1.0 wt %. Specifically, the YP of PNWBDF is 46.5 lb/100 ft^2 at the 1.0 wt % of P-Al_2O_3 NPs, which is 18% more than the YP of SNWBDF at equivalent concentrations of S-Al_2O_3 NPs.

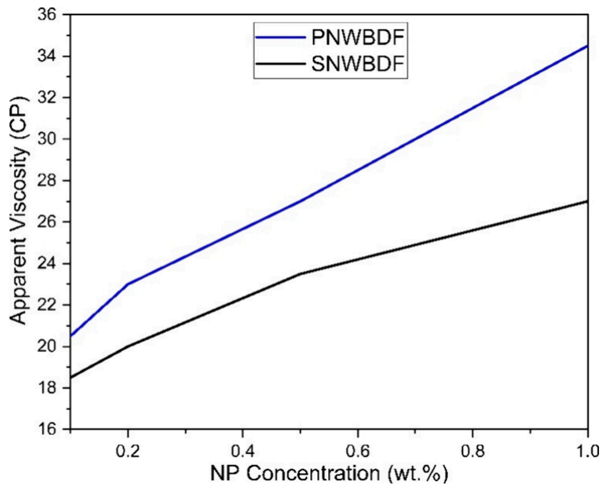

Figure 9. Apparent viscosity at different concentrations of P-Al_2O_3 and S-Al_2O_3 NPs.

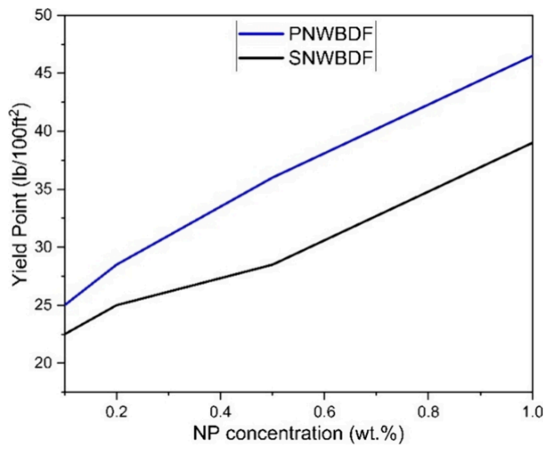

Figure 10. Yield point at different concentrations of P-Al_2O_3 and S-Al_2O_3 NPs.

The reason behind this phenomenon is the stronger van der Waals forces and lower electrostatic repulsion among the P-Al_2O_3 NPs.

Gel Strength. Gel strength is a crucial property of drilling fluids that indicates their ability to suspend solids and cuttings.[43] Gel strength is the properties of the drilling fluid measured when the circulation system is halted. Figures 10 and 11 illustrate the effects of P-Al_2O_3 and S-Al_2O_3 NPs on the gel strength of PNWBDF and SNWBDF at different concentrations after 10 s and 10 min, respectively.

Initially, the base mud exhibited gel strength values of 12 lb/100 ft^2 at 10 s and 13.5 lb/100 ft^2 at 10 min. As shown in Figures 11 and 12, the 10 s and 10 min gel strengths increased with the addition of P-Al_2O_3 and S-Al_2O_3 NPs. The 10 s and 10 min gel strengths of PNWBDF were 44.5 and 77 lb/100 ft^2 at 1.0 wt % of P-Al_2O_3 NPs, respectively, which is about 30% more than gel strengths achieved by S-Al_2O_3 NPs at the same concentration. This difference is attributed to the dispersion instability of P-Al_2O_3 NPs, while S-Al_2O_3 NPs exhibit greater stability in solution.

Effect of P-Al_2O_3 and S-Al_2O_3 NPs on the Filtration Properties of WBDF. *Filtration Loss.* The fluid loss is pertinent to the volume of fluid, which is lost into the formation due to a permeable mud cake.[44] In drilling

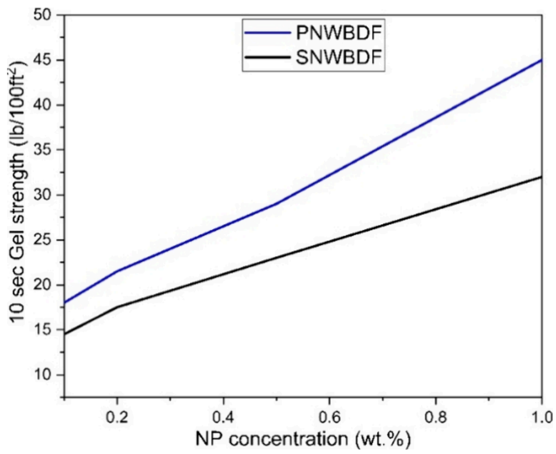

Figure 11. 10_{sec} gel strength at different concentrations of P-Al_2O_3 and S-Al_2O_3 NPs.

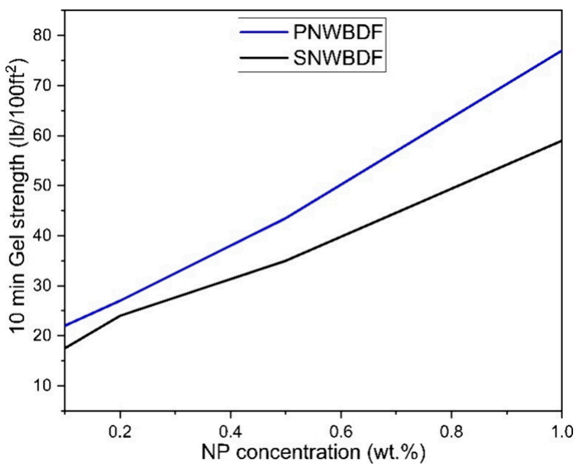

Figure 12. 10_{min} gel strength at different concentrations of P-Al_2O_3 and S-Al_2O_3 NPs.

operations, the high fluid loss is considered unfavorable.[45] The base mud without NPs showed a fluid loss of 14.0 mL after 30 min (Figure 13). The fluid loss at 1.0 wt % of P-Al_2O_3 NPs is 24.5 mL, which is 26% more than the fluid loss caused by S-Al_2O_3 NPs at the same concentration. The reduced fluid loss in

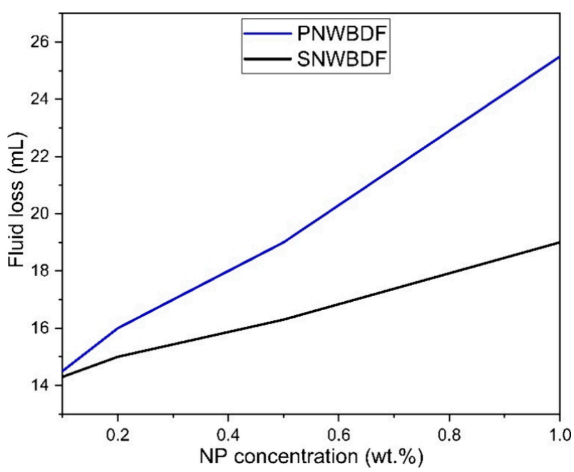

Figure 13. Fluid loss at different concentrations of P-Al_2O_3 and S-Al_2O_3 NPs.

SNWBDF is attributed to the effective dispersion of the S-Al_2O_3 NPs. This dispersion allows the NPs to block nano- and microscale pore spaces in the mud cake, reducing its permeability and consequently lowering fluid loss.

Quality and Thickness of the Filter Cake. For optimum drilling fluid, it is desired that the drilling fluid should form a thin and impermeable mud cake around the walls of the wellbore to have minimal fluid loss volume and sustain the wellbore stability.[46−48] The base fluid produced a mud cake with a thickness of 5 mm. Tables 2 and 3 show that the P-

Table 2. Permeability of the Mud Cake Formed by Pristine Nano Bentonite Water-Based Drilling Fluids (ΔP = 7.1 atm, A = 124.8 cm^2)

concentration (wt %)	h_{mc} (cm)	μ (cP)	dv_f/dt (cm^3/s)	K (mD)
0	0.5	6	0.0065	0.0220
0.1	0.4	7.5	0.0062	0.0210
0.2	0.48	9	0.0058	0.0283
0.5	0.5	11	0.0051	0.0317
1.0	0.53	12.5	0.0045	0.0350

Table 3. Permeability of the Mud Cake Formed by Silanized Nano Bentonite Water-Based Drilling Fluids (ΔP = 7.1 atm, A = 124.8 cm^2)

concentration (wt %)	h_{mc} (cm)	μ (cP)	dv_f/dt (cm^3/s)	K (mD)
0	0.5	6	0.0065	0.0220
0.1	0.38	6.8	0.0059	0.0172
0.2	0.43	8	0.0055	0.0213
0.5	0.45	9.5	0.0048	0.0232
1.0	0.48	10.6	0.0041	0.0236

Al_2O_3 NPs formed a thicker and permeable mud cake as compared to the thinner and impermeable cake formed by S-Al_2O_3 NPs at the same concentrations. This behavior, illustrating the pore-plugging capabilities of both pristine and silane-coated NPs, is depicted in Figure 14. It was observed that S-Al_2O_3 NPs produce a thinner cake due to the effective plugging of nano- and microsized pore spaces. In contrast, P-Al_2O_3 NPs form a thicker and less effectively plugged cake due to particle agglomeration.

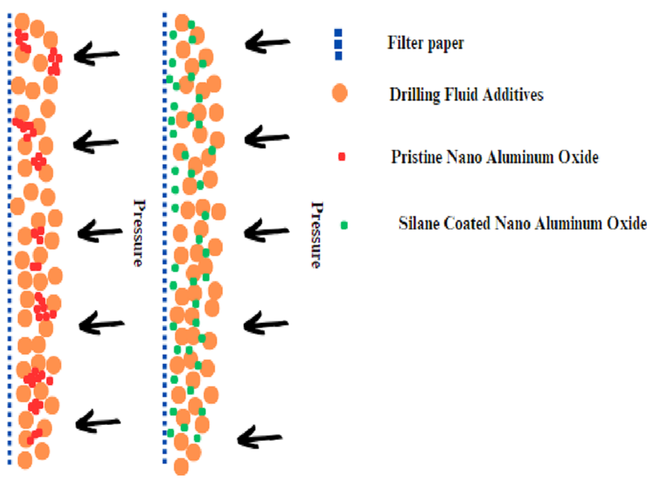

Figure 14. Dispersion and agglomeration of P-Al_2O_3 and S-Al_2O_3 NPs at the mud cake.

https://doi.org/10.1021/acsomega.4c08116
ACS Omega 2025, 10, 955−963

Mud Cake Permeability. Permeability is the ability of a medium to transmit the fluid. In drilling operations, it is intended to make an impermeable mud cake; however, it is not possible. Therefore, it is endeavored to develop a drilling fluid that should make a thin and less permeable mud cake.

Darcy's law (eq viii) was used to determine the permeability of the filter cake.

$$dv_f/dt = KA\Delta P/\mu h_{mc} \quad \text{(viii)}$$

where h_{mc} is the thickness of the mud cake (cm), μ is the viscosity of the mud filtrate (cP), dv_f/dt is the filtration rate (cm^3/s), and K is the permeability of the mud cake (millidarcy, mD). Tables 2 and 3 present the calculated permeabilities of the mud cakes. For PNWBDF, the permeability of the mud cake at a high concentration of 1.0 wt % was 0.0350 mD, whereas the permeability of the filter cake from SNWBDF at the same amount was 0.0236 mD.

CONCLUSIONS

In this study, pristine aluminum oxide (P-Al_2O_3) NPs were silanized by using APTES to create silane-coated aluminum oxide (S-Al_2O_3) NPs. Characterization using FTIR, XRD, and SEM confirmed the successful synthesis of the NPs and the effective coupling of APTES with Al_2O_3. Following this, nanoenhanced bentonite water-based drilling fluids (BWBDF) were formulated by incorporating various concentrations (ranging from 0.1 to 1.0 wt %) of P-Al_2O_3 and S-Al_2O_3 NPs.

The S-Al_2O_3 NPs displayed significantly enhanced pseudoplastic behavior in comparison to P-Al_2O_3 at the maximum concentration of 1.0 wt %. At this concentration, S-Al_2O_3 NPs reduced the PV of the drilling mud by 30% relative to P-Al_2O_3, demonstrating their effectiveness in managing flow resistance. Additionally, the S-Al_2O_3 NPs decreased the apparent viscosity of the drilling fluid by 30%, indicating improved fluid efficiency and reduced energy requirements. The YP was similarly affected, with S-Al_2O_3 reducing it by 18% at the same concentration, highlighting its potential in stabilizing drilling operations. Gel strength—measured at both 10 s and 10 min—was reduced by 37% with S-Al_2O_3 NPs compared to P-Al_2O_3, which can lead to easier restarting of circulation after shut-in periods. Furthermore, S-Al_2O_3 NPs showed superior filtration performance, evidenced by reductions in fluid loss and the formation of a thinner, less permeable mud cake. Specifically, at 1.0 wt %, S-Al_2O_3 reduced filtrate loss by 26%, decreased mud cake thickness by 10%, and lowered mud cake permeability by 48% compared to P-Al_2O_3.

In conclusion, the silane-coated aluminum oxide NPs presented superior performance over pristine aluminum oxide NPs, in controlling the rheology and filtration efficiency. Therefore, S-Al_2O_3 NPs are promising additives for optimizing water-based drilling fluid performance, especially for challenging drilling environments. Future studies should explore the effects of these NPs under high-temperature, high-pressure conditions to further validate these findings and extend their applicability.

AUTHOR INFORMATION

Corresponding Author

Abdul Haque Tunio − *Institute of Petroleum and Natural Gas Engineering, Mehran University of Engineering and Technology, Jamshoro, Sindh 77150, Pakistan;* Email: haque.tunio@faculty.muet.edu.pk

Authors

Imran Ahmed Hullio − *Institute of Petroleum and Natural Gas Engineering, Mehran University of Engineering and Technology, Jamshoro, Sindh 77150, Pakistan;* orcid.org/0000-0002-0305-1749

Waseem Akhtar − *Department of Metallurgy & Materials Engineering, Mehran University of Engineering and Technology, Jamshoro, Sindh 76062, Pakistan*

Muddassir Ali Memon − *Department of Metallurgy & Materials Engineering, Mehran University of Engineering and Technology, Jamshoro, Sindh 76062, Pakistan*

Nasir Mehmood Gabol − *Department of Metallurgy & Materials Engineering, Mehran University of Engineering and Technology, Jamshoro, Sindh 76062, Pakistan*

Complete contact information is available at: https://pubs.acs.org/10.1021/acsomega.4c08116

Notes

The authors declare no competing financial interest.

ACKNOWLEDGMENTS

The authors would like to gratefully acknowledge Mehran University of Engineering and Technology (MUET), Jamshoro, Sindh, Pakistan, for financial support of this research.

REFERENCES

(1) Bridges, S.; Robinson, L. H. a practical handbook for drilling fluids processing, *Gulf Professional*, **2020**, https://www.elsevier.com/books/a-practical-handbook-for-drilling-fluids-processing/bridges/978-0-12-821341-4.

(2) Kariman Moghaddam, A.; Davoodi, S.; Ramazani S.A, A.; Minaev, K. M. Mesoscopic theoretical modeling and experimental study of rheological behavior of water-based drilling fluid containing associative synthetic polymer, bentonite, and limestone. *J. Mol. Liq.* **2022**, *347*, No. 117950.

(3) Paixão, M. V. G.; da Silva Fernandes, R.; de Souza, E. A.; de Carvalho Balaban, R. Thermal energy storage technology to control rheological properties of drilling fluid. *J. Mol. Liq.* **2021**, *341*, No. 116931.

(4) Foxenberg, W. E.; Ali, S. A.; Long, T. P.; Vian, J. Field experience shows that new lubricant reduces friction and improves formation compatibility and environmental impact. *SPE international symposium and exhibition on formation damage control*; Society of Petroleum Engineers; **2008**, January.

(5) Al Jaberi, J.; Bageri, B.; Elkatatny, S.; Patil, S. Primary Investigation of Barite-Weighted Water-Based Drilling Fluid Properties. *ACS Omega* **2023**, *8* (2), 2155−2163.

(6) Skalle, P.*Drilling fluid engineering*. 3rd; E-Publishing Inc.: London; 2012.

(7) Zhu, W.; Zheng, X. Effective Modified Xanthan Gum Fluid Loss Agent for High-Temperature Water-Based Drilling Fluid and the Filtration Control Mechanism. *ACS Omega* **2021**, *6* (37), 23788−23801.

(8) Sayindla, S.; Lund, B.; Ytrehus, J. D.; Saasen, A. Hole cleaning performance comparison of oil-based and water-based drilling fluids. *J. Pet. Sci. Eng.* **2017**, *159* (49), 49.

(9) Mansour, A.; Dahi Taleghani, A.; Salehi, S.; Li, G.; Ezeakacha, C. Smart lost circulation materials for productive zones. *Journal of Exploration & Production Technology* **2019**, *9*, 281−296.

(10) Sajjadian, M.; Sajjadian, V. A.; Rashidi, A. Experimental evaluation of nanomaterials to improve drilling fluid properties of water-based muds HP/ HT applications. *J. Petrol. Sci. Eng.* **2020**, *190*, No. 107006.

(11) Ibrahim, M. A.; Jaafar, M. Z.; Md Yusof, M. A.; Idris, A. K. A review on the effect of nanoparticle in drilling fluid on filtration and formation damage. *J. Pet. Sci. Eng.* **2022**, No. 110922.

(12) Karakosta, K.; Mitropoulos, A. C.; Kyzas, G. Z. a review in nanopolymers for drilling fluids applications. *J. Mol. Struct.* **2021**, *1227*, No. 129702. Article
(13) Abdo, J.; Haneef, M. D. Clay Nanoparticles Modified Drilling Fluids for Drilling of Deep Hydrocarbon Wells. *Appl. Clay Sci.* **2013**, *86*, 76−82.
(14) Ismail, A. R.; Rashid, N. M.; Jaafar, M. Z.; Sulaiman, W. R. W.; Buang, N. A. Effect of Nanomaterial on the Rheology of Drilling Fluids. *J. Appl. Sci.* **2014**, *14* (11), 1192−1197.
(15) Zamora-Ledezma, C.; Narvéez-Muñoz, C.; Guerrero, V. H.; Medina, E.; Meseguer-Olmo, L. Nanofluid Formulations Based on Two-Dimensional Nanoparticles, Their Performance, and Potential Application as Water-Based Drilling Fluids. *ACS. Omega* **2022**, *7* (24), 20457−20476.
(16) Cheraghian, G. Nanoparticles in drilling fluid: A review of the state-of-the-art. *J.Mater. Res. Technol.* **2021**, *13*, 737−753.
(17) Cai, J.; Chenevert, M. E.; Sharma, M. M.; et al. Decreasing Water Invasion into Atoka Shale Using Nanomodified Silica Nanoparticles. *SPE Drill & Compl* **2012**, *27* (1), 103−112.
(18) Clavijo, J. V.; Roldán, L. J.; Valencia, L.; Lopera, S. H.; Zabala, R. D.; Cárdenas, J. C.; Durán, W.; Franco, C. A.; Cortés, F. B. Influence of size and surface acidity of silica nanoparticles on inhibition of the formation damage by bentonite-free water-based drilling fluids, Part II: dynamic filtration. *Advances in Natural Sciences: Nanoscience and Nanotechnology.* **2020**, *11* (1), No. 015011.
(19) Contreras, O.; Hareland, G.; Husein, M.et al.2014. *Application of In-House Prepared Nanoparticles as Filtration Control Additive to Reduce Formation Damage.* Presented at the International Symposium and Exhibition on Formation Damage Control: Lafayette, LA, 26−28 February. SPE-168116-MS. .
(20) William, J. K. M.; Ponmani, S.; Samuel, R.; Nagarajan, R.; Sangwai, J. S. Effect of CuO and ZnO nano fluids in xanthan gum on thermal, electrical and high pressure rheology of Water-based drilling fluids. Journal of Petroleum Science. *Engineering* **2014**, *117*, 15.
(21) Ahasan, M. H.; Alahi Alvi, M. F.; Ahmed, N.; Alam, M. S. An investigation of the effects of synthesized zinc oxide nanoparticles on the properties of water-based drilling fluid. *Pet. Res.* **2022**, *7*, 131.
(22) Dejtaradon, P.; Hamidi, H.; Chuks, M. H.; Wilkinson, D.; Rafati, R. Impact of ZnO and CuO nano particles on the rheological and filtration properties of water based drilling fluid. *Colloids Surf., A* **2019**, *570*, 354−367.
(23) Alam, M. S.; Ahmed, N.; Salam, M. A. Study on rheology and filtration properties of field used mud using iron (III) oxide nanoparticles. *Upstream Oil Gas Technol.* **2021**, *7*, No. 100038.
(24) Bayat, A. E.; Jalalat Moghanloo, P.; Piroozian, A.; Rafati, R. Roozbeh Rafatib, Experimental investigation of rheological and filtration properties of waterbased drilling fluids in presence of various nanoparticles. *Colloids Surf., A* **2018**, *555*, 256−263.
(25) Gohari, B.; Abu-Zahra, N. Polyethersulfone Membranes Prepared with 3-Aminopropyltriethoxysilane Modified Alumina Nanoparticles for Cu(II) Removal from Water. *ACS Omega* **2018**, *3* (8), 10154−10162.
(26) Wang, Z.; Wu, Y.; Luo, P.; Tian, Y.; Lin, Y.; Guo, Q. Poly (sodium pstyrene sulfonate) modified Fe_3O_4 nanoparticles as effective additives in water-based drilling fluids. *J. Pet. Sci. Eng.* **2018**, *165*, 786−797.
(27) Wu, Y.; Wang, Z.; Yan, Z.; Zhang, T.; Bai, Y.; Wang, P.; Luo, P.; Gou, S.; Guo, Q. Q, Guo, Zhang, Poly (2-acrylamide-2-methylpropanesulfonic acid) modified SiO_2 nano particles for water based drilling fluids. *Ind. Eng. Chem. Res.* **2017**, *56*, 168−174.
(28) Abbas, G.; Tunio, A. H.; Memon, K. R.; Mahesar, A. A.; Memon, F. H.; Abbasi, G. R. Abdul Haque Tunio, Khalil Rehman Memon, Aftab Ahmed Mahesar, Faisal Hussain Memon, and Ghazanfer Raza Abbasi, "Modification of Cellulose Ether with Organic Carbonate for Enhanced Thermal and Rheological Properties: Characterization and Analysis. *ACS Omega* **2023**, *8* (28), 25453−25466.
(29) Smith, S. R.; Rafati, R.; Sharifi Haddad, A.; Cooper, A.; Hamidi, H. Application of aluminium oxide nanoparticles to enhance rheological and filtration properties of water based muds at HPHT conditions. *Colloids Surf., A* **2018**, *537*, 361−371.
(30) Naayi, Saif A.; Hassan, Azhar I.; Salim, Evan T. FTIR and X-ray diffraction analysis of Al2O3 nanostructured thin film prepared at low temperature using Spray pyrolysis method, *International Journal of Nano electronics and Materials.*
(31) Shivanand, F. Magdaline Eljeeva Emerald and Somveer, "Synthesis and characterization of aluminum oxide nanoparticles. *Pharma Innov. J.* **2022**, *11* (6), 1068−1072.
(32) Srungavarapu, M.; Patidar, K. K.; Pathak, A. K.; Mandal, A. Performance studies of water-based drilling fluid for drilling through hydrate bearing sediments. *Appl. Clay Sci.* **2018**, *152*, 211−220.
(33) William, J. K. M.; Ponmani, S.; Samuel, R.; Nagarajan, R.; Sangwai, J. S. Effect of CuO and ZnO nanofluids in xanthan gum on thermal, electrical and high pressure rheology of water-based drilling fluids. *J. Pet. Sci. Eng.* **2014**, *117*, 15−27.
(34) Piroozian, A.; Ismail, I.; Yaacob, Z.; Babakhani, P.; Ismail, A. S. I. Impact of drilling fluid viscosity, velocity and hole inclination on cuttings transport in horizontal and highly deviated wells. *J. Pet. Explor. Prod. Technol.* **2012**, *2* (3), 149−156.
(35) Abbas, G.; Tunio, A. H.; Memon, K. R.; Mahesar, A. A.; Memon, F. H. Abdul Haque Tunio, Khalil Rehman Memon, Aftab Ahmed Mahesar, and Faisal Hussain Memon, "Effect of Temperature and Alkali Solution to Activate Diethyl Carbonate for Improving Rheological Properties of Modified Hydroxyethyl Methyl Cellulose. *ACS Omega* **2024**, *9* (4), 4540−4554.
(36) Aftab, A. A. R. I.; Ismail, A. R.; Ibupoto, Z. H.; Akeiber, H.; Malghani, M. G. K. Nanoparticles based drilling muds a solution to drill elevated temperature wells: a review. *Renew. Sustain. Energy Rev.* **2017**, *76*, 1301−1313.
(37) Ridha, S.; Ibrahim, A.; Shahari, R.; Fonna, S. Graphene nanoplatelets as high- performance filtration control material in water-based drilling fluids. *J. Mater. Sci. Eng.* **2018**, *352* (1), No. 012025.
(38) Novara, R.; Rafati, R.; Sharifi Haddad, A. Rheological and filtration property evaluations of the nano-based muds for drilling applications in low temperature environments. *Colloids Surf.* **2021**, *A 622*, No. 126632.
(39) Boyou, N. V.; Ismail, I.; Wan Sulaiman, W. R.; Sharifi Haddad, A.; Husein, N.; Hui, H. T.; Nadaraja, K. Experimental investigation of hole cleaning in directional drilling by using nano-enhanced water-based drilling fluids. *J. Petrol. Sci. Eng.* **2019**, *176*, 220−231.
(40) Saadoon Al-Yasiri, M.; Tareq Al-Sallami, W. How the drilling fluids can be made more efficient by using nanomaterials. *Am. J. Nano Res. Appl.* **2015**, *3*, 41−45.
(41) Güneyisi, E.; Gesoglu, M.; Algın, Z.; Yazıcı, H. Rheological and fresh properties of self- compacting concretes containing coarse and fine recycled concrete aggregates. *Constr. Build. Mater.* **2016**, *113*, 622−630.
(42) Bageri, B. S.; Gamal, H.; Elkatatny, S.; Patil, S. Effect of Different Weighting Agents on Drilling Fluids and Filter Cake Properties in Sandstone Formations. *ACS Omega* **2021**, *6* (24), 16176−16186.
(43) Noah, A. Z.; El Semary, M. A.; Youssef, A. M.; El-Safty, M. A. Enhancement of yield point at high pressure high temperature wells by using polymer nanocomposites based on ZnO & CaCO3 nanoparticles. *Egypt. J. Pet.* **2017**, *26* (1), 33−40.
(44) Ramesh, K. T. *Nanomaterials: Mechanics and Mechanisms*, Chapter 2 Springer, 978−0-387−09783−1, 2001.
(45) Rafati, R.; Smith, S. R.; Sharifi Haddad, A.; Novara, R.; Hamidi, H. Effect of nanoparticles on the modifications of drilling fluids properties: a review of recent advances. *J. Pet. Sci. Eng.* **2018**, *161*, 61−76.
(46) Al-Mahdawi, F. H. M.; Saad, K. Enhancement of drilling fluid properties using nanoparticles. *Iraqi J. Chem. Pet. Eng.* **2018**, *19*, 21−26.
(47) Adebayo, A. R.; Bageri, B. S. A simple NMR methodology for evaluating filter cake properties and drilling fluid-induced formation damage. *J. Pet. Explor. Prod. Technol.* **2020**, *10* (4), 1643−1655.

(48) Saboori, R.; Sabbaghi, S.; Kalantariasl, A. Improvement of rheological, filtration and thermal conductivity of bentonite drilling fluid using copper oxide/ polyacrylamide nanocomposite. *J. Powder Technol.* **2019**, *353*, 257−266.

https://doi.org/10.1021/acsomega.4c08116
ACS Omega 2025, 10, 955−963